ORIGINAL PAPER

Structural and Electrical Properties of Ni-Co Nanoferrites Prepared by Co-precipitation Route

**Asghari Maqsood · Kishwar Khan ·
M. Anis-ur-Rehman · Muhammad Ali Malik**

Abstract A series of $Ni_{1-x}Co_xFe_2O_4$ ($x = 0.1$, 0.2, 0.3, 0.4, 0.5) spinel ferrites have been synthesized successfully using the chemical co-precipitation route. The materials were characterized by X-rays powder diffractometry (XRD) and the electrical properties. The obtained crystallite size variation was within 15 to 33 nm using the Scherrer formula. The dc electrical resistivity was measured as a function of temperature. It is noticed that σ_{dc} increases with a rise in temperature. The dielectric measurements were carried out at room temperature as a function of frequency and composition (x). The dielectric constant (ε') and dielectric loss tangent ($\tan\delta$) showed a decreasing trend with increasing field frequency. The ac electrical conductivity is calculated from the dielectric measurements; it increases with the rise in frequency.

Keywords DC electrical conductivity · Nanoferrites · Porosity

1 Introduction

Synthesis of nano-sized spinel ferrites has become an interesting field of modern research. These nano-sized parti-

cles can be prepared by various methods like hydrothermal, microwave-hydrothermal, co-precipitation, combustion, sol-gel, precursor, spray drying and freeze drying, micro emulsion, reverse micelle method etc. [1–3]. Ni-Co ferrite is one of the important magnetic materials for many high-frequency applications. This is because of its better properties at higher frequencies (high resistivity, high Curie point, environmental stability, low cost) and lower densification temperature than that of presently used Ni-Co ferrite [4–6]. Therefore, in the present investigation, a detailed study is undertaken.

2 Experimental Procedure

2.1 Preparation of Materials

The polycrystalline powders of series $Ni_{1-x}Co_xFe_2O_4$ ($0.0 \leq x \leq 0.5$) in steps of 0.1 were prepared by the chemical co-precipitation route. All the chemicals were of analytical grade. The co-precipitating aqueous solutions of $Ni(NO_3)_2 \cdot 6H_2O$, $Co(NO_3)_2 \cdot 6H_2O$ and $Fe(NO_3)_3 \cdot 9H_2O$ mixtures, respectively, were prepared in alkaline medium. The molarity of the co-precipitating agent (NaOH) used was 3 mol/l. The solutions of $Ni(NO_3)_2 \cdot 6H_2O$ 150 ml of 0.1 M and $Fe(NO_3)_3 \cdot 9H_2O$ in their stoichiometry, 150 ml of 0.2 M $Co(NO_3)_2 \cdot 6H_2O$, $Ni(NO_3)_2 \cdot 6H_2O$ and 150 ml of 0.05 M $Co(NO_3)_3 \cdot 6H_2O$ in the case of $Ni_{(0.5)}Co_{(0.5)}Fe_2O_4$ and similarly for the other values of x were dissolved in distilled water with a constant stirring by a magnetic stirrer, until a clear solution was obtained. To obtain ferrites of a smaller size, less dispersed in size and more chemically homogeneous, the mixing of reagents was performed as fast as possible by adding the precipitating reagent (NaOH) quickly into the metal solutions, contained in a beaker, with constant

A. Maqsood (✉) · K. Khan
Thermal Transport Laboratory, School of Chemical and Materials Engineering (SCME), National University of Sciences and Technology (NUST), Islamabad 45320, Pakistan
e-mail: tpl.qau@usa.net

K. Khan
e-mail: kishwar.nust@gmail.com

M. Anis-ur-Rehman · M. Ali Malik
Applied Thermal Physics Laboratory, Department of Physics, COMSATS Institute of Information Technology, Islamabad 44000, Pakistan

stirring until co-precipitation occurred. For the transformation of hydroxides into ferrites (dehydration and atomic rearrangement involved in the conversion of intermediate hydroxide phase into ferrites) it was required to maintain a temperature of 85 °C for 50 min. The pH of the reactions was kept between 11 and 11.5. The precipitates were thoroughly washed with distilled water until the washings were free from sodium and chloride ions. The product was dried in an electric oven at 105 °C for overnight to remove water contents. Ferrite powders were pelletized in circular disks by applying a uniaxial load using hydraulic press.

2.2 Measurements

The structure was determined through the X-ray diffraction (XRD) analysis. XRD patterns were taken using Cu $K\alpha$ ($\lambda = 1.5406$ Å) radiation at room temperature. The estimated crystallite size, lattice parameter, mass density, X-ray density and porosity were calculated using simple formulas [7, 8]. The dc electrical resistivity was obtained by a simple two-probe method within temperature range 300–650 K. The relation between resistivity and temperature [9] may be expressed as

$$\rho = \rho_0 \mathrm{Exp}(\Delta E / k_\mathrm{B} T) \tag{1}$$

where ΔE is the activation energy in (eV) for conduction, k_B is the Boltzmann constant and T is the temperature in Kelvin (K).

The drift mobility (μ_d) was calculated using the equation [10]

$$\mu_\mathrm{d} = 1/ne\rho \tag{2}$$

where ρ is the resistivity, e is the charge on electron and n is the concentration of charge carrier which can be calculated from the relation [11]

$$n = N_\mathrm{a} D_\mathrm{m} P_\mathrm{Fe} / M \tag{3}$$

where N_a, D_m and M are the Avogadro's number, mass density and molecular weight of the corresponding sample, respectively, and P_Fe is the number of iron atoms in the formula $\mathrm{Ni}_{1-x}\mathrm{Co}_x\mathrm{Fe}_2\mathrm{O}_4$. The value of the dielectric constant was calculated using the relation between the capacitance, ε_0, and the dimensions of the sample. The capacitance and dielectric loss were recorded simultaneously using a WAYNE KERR LCR METER (6440B) in the frequency range from 100 Hz to 3 MHz at room temperature. The samples were pressed into circular disc shaped pellets, and silver coating was done on adjacent faces to make the parallel plate capacitor geometry with ferrite material as the dielectric medium. The real part of the dielectric constant (ε') was calculated by the relation [7, 11]

$$\varepsilon' = Cd/\varepsilon_0 A \tag{4}$$

where C is the capacitance in Farad, d the thickness of the pellets in m, A the cross-sectional area of a flat surface of the pellet sample in m^2 and where ε_0 is the permittivity of free space, equal to 8.854×10^{-12} F/m. The dielectric loss tangent (tan δ) can be determined in terms of real and imaginary parts of dielectric constant as

$$\tan\delta = D = \varepsilon''/\varepsilon' \tag{5}$$

The ac conductivity was calculated from dielectric constant and dielectric loss tangent (tan δ) as $\sigma_\mathrm{ac} = \omega\varepsilon_0\varepsilon' \tan\delta$, where σ_ac is the ac conductivity, ω is the angular frequency, ε_0 is the permittivity of free space; ε' is the dielectric constant and tan δ is the dielectric loss factor of the samples.

2.3 Results and Discussion

Nano-crystalline $\mathrm{Ni}_{1-x}\mathrm{Co}_x\mathrm{Fe}_2\mathrm{O}_4$ ferrites with ($0.0 \leq x \leq 0.5$) showed a cubic spinel structure from its XRD pattern (Fig. 1). The particle size of the nano-crystalline precipitates was estimated by Scherrer formula [7]. The particle size remained within the range 15 to 33 nm for the studied compositions. The lattice constant a, measured density D_m, X-ray density D_x and porosity P as a function of cobalt concentration are tabulated in Table 1. It is noticed that the lattice constant increased with the cobalt concentration in the lattice. This is due to the radius of the cobalt ions (0.78 Å). Addition of cobalt at the expense of Ni in the ferrite is expected to increase the lattice constant. The variation of porosity with Co concentration is also tabulated in Table 1. It is observed that porosity decreased as the concentration of Co increased; again it is due to the larger ionic radius of cobalt compared to Ni. The diameter of the nanoparticles along with the measured density corresponding to cobalt concentration is given in Table 1. The measured density (D_m) of the corresponding materials ranges from 2.79 to 3.52 g cm^{-3}.

2.4 Electrical Properties

The study of the electrical and dielectric properties give valuable information about the behavior of electric charge carriers which leads to good understanding and explanation of conduction mechanism in ferrites. The electrical resistivity is one of the important properties of ferrites, particularly for high-frequency applications. The resistivity of the ferrites, in general, depends on several factors such as the density, porosity, grain size, chemical composition, etc. Figure 2 illustrates the variation of dc electrical resistivity of $\mathrm{Ni}_{(1-x)}\mathrm{Co}_{(x)}\mathrm{Fe}_2\mathrm{O}_4$ measured as a function of temperature. The measured DC resistivity was found for sample $x = 0.0$, at 573 K is 1.73×10^5 Ω cm and for sample $x = 0.1$, 2.09×10^5 Ω cm as given in Table 1. From Fig. 2, it is evident that DC electrical resistivity exhibits semiconduc-

Table 1 The estimated crystallite size for (3 1 1) peak, lattice parameter (a), lattice volume (V), mass density (D_m), X-ray density (D_x), porosity (P), dc electrical resistivity (ρ), drift mobility (μ_d), activation energy (ΔE), correlation co-efficient (R), dielectric constant (ε'), dielectric loss ($\tan\delta$) and ac conductivity (σ_{ac}) of $Ni_{1-x}Co_xFe_2O_4$ nanoferrites

Parameters	Cobalt concentration					
	$x = 0.0$	$x = 0.1$	$x = 0.2$	$x = 0.3$	$x = 0.4$	$x = 0.5$
t (311) (nm)	17.1	21.3	15.5	24.9	22.9	33.4
a (Å)	8.335	8.341	8.342	8.344	8.345	8.346
V (Å^3)	579	580	580	581	581	581
D_m (g/cm^3)	2.79	2.88	2.98	3.20	3.47	3.52
D_x (g/cm^3)	5.37	5.36	5.36	5.36	5.36	5.35
P (fraction)	0.48	0.46	0.44	0.40	0.35	0.34
ρ (Ω cm) at 573 K	1.73×10^5	1.73×10^5	1.73×10^5	1.73×10^5	1.73×10^5	1.73×10^5
μ_d (cm^2 V s) at 573 K	2.07×10^{-9}	2.07×10^{-9}	1.88×10^{-9}	1.63×10^{-9}	1.60×10^{-9}	1.29×10^{-9}
σ_{ac} (S m^{-1}) at 573 K	1.51×10^{-3}	9.56×10^{-4}	9.65×10^{-4}	4.78×10^{-4}	5.92×10^{-4}	9.14×10^{-4}
σ_{dc} (S m^{-1}) at 573 K	3.24×10^{-6}	4.78×10^{-6}	3.25×10^{-6}	3.25×10^{-6}	2.94×10^{-6}	2.35×10^{-6}
ΔE (eV)	0.169	0.217	0.242	0.265	0.280	0.283
R	0.9998	0.9997	0.9993	0.9998	0.9998	0.9996
ε' at 1 MHz	39.9121	21.9782	28.6513	15.1013	18.7571	30.0096
ε' at 3 MHz	28.7787	15.6873	20.0090	10.8035	13.3270	13.2617
$\tan\delta$ at 3 MHz	0.0015	0.3145	0.3655	0.4212	0.6665	0.8755

tor like behavior, i.e. decreasing resistivity with increasing temperature for all the samples. The conduction mechanism in these ferrites can be explained by a hopping mechanism [12, 13].

The activation energy of all the samples was determined from the slope of the $\ln\rho$ versus $(1/k_B T)$. The activation energy (ΔE) of the studied specimens was found within the range 0.16–0.28 (eV) with a maximum value for $x = 0.1$. The values of activation energy are in good agreement with previously reported values for other spinal ferrites [13, 14].

The drift mobility for all the samples has been calculated using (2) and (3). The plots of (μ_d) with reciprocal temperature are shown in Fig. 3. The temperature variation of resistivity in this case was mainly attributed to change of drift mobility with temperature rather than to the variation of charge carrier concentration. According to the hopping model, electrons are strongly localized on the cations. The localization may be attributed to electron phonon interaction. An additional localization of electron at Fe^{+2} ions is over octahedral site in the spinel lattice [15]. It is observed from the graph that by increasing temperature, the drift mobility also increases. It may be due to the fact that the charge carriers start hopping from one site to another as the temperature increases.

The σ_{dc} as a function of temperature is shown in Fig. 4. It is noticed that σ_{dc} increased with a rise in temperature. The value of σ_{dc} (S m^{-1}) at 573 K for nano-crystalline $Ni_{1-x}Co_xFe_2O_4$ is listed in Table 1. Figure 4 shows that the dc conductivity increased with increase in temperature for all the samples, in agreement with the literature. Spinel

ferrites are known to have semiconducting-like behavior. In all the plots a change in slope at a particular temperature occurs. Generally, the change of slope is attributed to a change in conductivity mechanism.

2.5 Dielectric Properties

The dielectric behavior is one of the most important characteristics of ferrites which markedly depend on the preparation conditions, e.g. sintering time and temperature, type and quantity of additives. The dielectric constant (ε') results are due to the heterogeneous structure of the material. The frequency dependence of the dielectric constant for all the samples is shown in Fig. 5, and it can be seen that all the samples showed similar behavior, i.e. dielectric constant decreased initially with increase in frequency and reached a constant value at higher frequency. After a certain increase in frequency all the samples exhibit a frequency-independent behavior, which can be explained on the basis of Maxwell–Wagner interfacial type polarization, which is in agreement with Koop's phenomenological theory [16, 17]. The dielectric polarization in ferrites is similar with the conduction hopping mechanism. Hopping between Fe^{2+} and Fe^{3+} the local displacement of electrons in the direction of the applied field occurs and these electrons determine the polarization. The polarization decreased with increasing frequency and then reached a constant value due to the fact that beyond a certain external field frequency, and as a result electron exchange $Fe^{2+} <=> Fe^{3+}$ cannot follow the alternating field. The large value of the dielectric constant at lower frequency
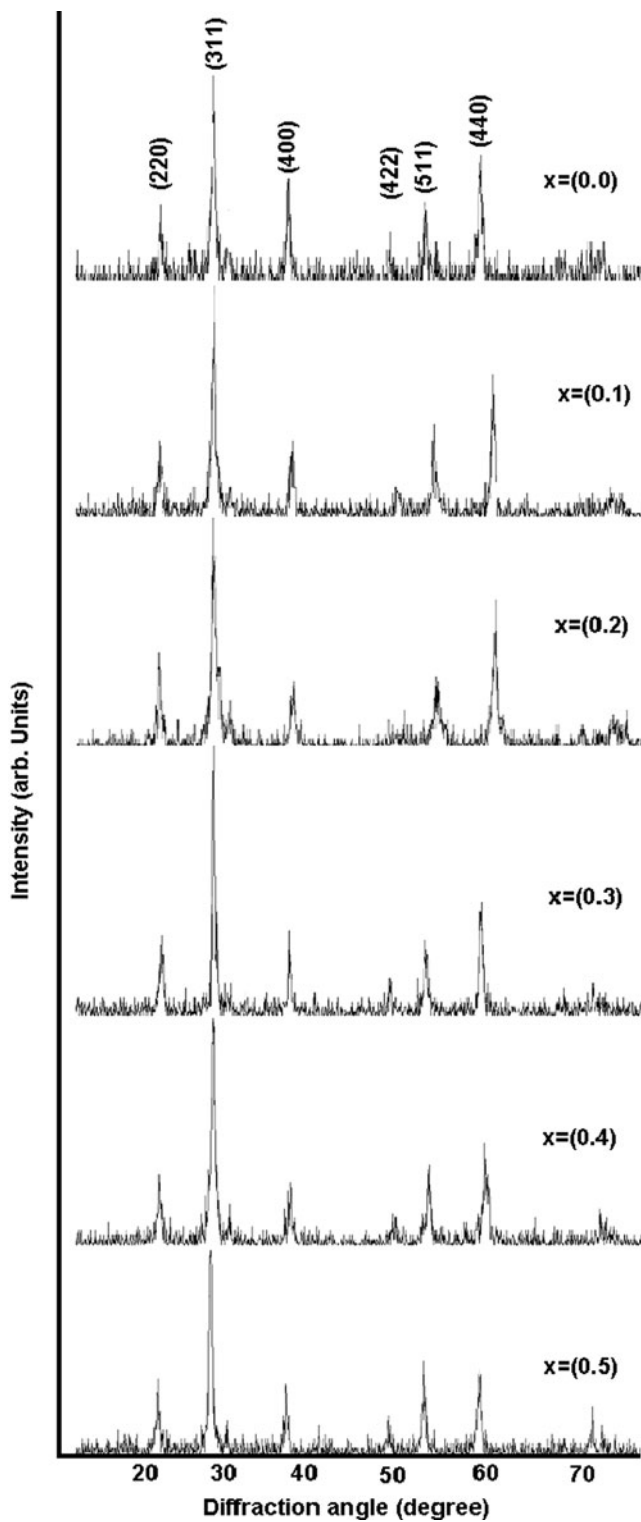
Fig. 1 Indexed X-ray pattern of $Ni_{1-x}Co_xFe_2O_4$

is due to the predominance of species like Fe^{2+} ions, interfacial dislocations piled up, oxygen vacancies, grain boundary defects, etc. [17, 18], while the decrease in ε' with frequency is natural because of the fact that any species contributing to
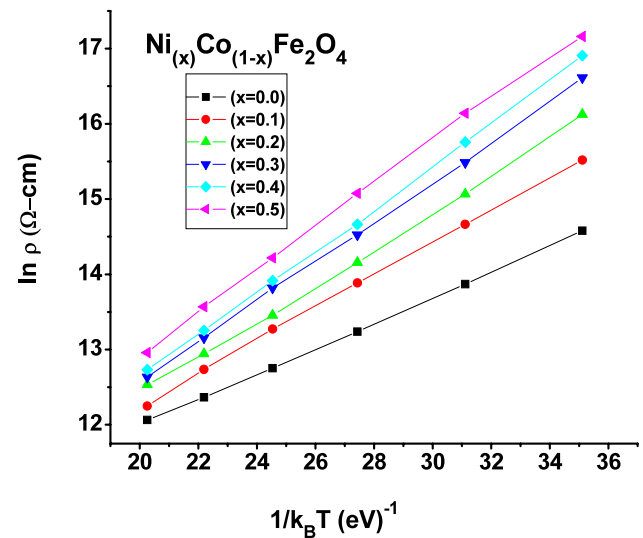

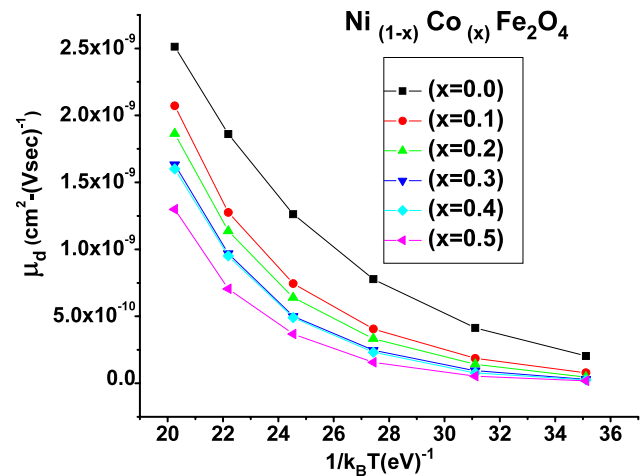**Fig. 2** Composition variation of dc electrical resistivity ($\ln \rho$) with $1/k_BT$ $(eV)^{-1}$

Fig. 3 Temperature dependence of drift mobility (μ_d) in $Ni_{1-x}Co_xFe_2O_4$ nanoferrites

polarizability is found to show lagging behind the applied field at some higher frequencies.

The dielectric loss tangent ($\tan \delta$) as a function of frequency is studied at room temperature. The plot of dielectric loss tangent or dielectric loss factor with frequency as Inf is depicted in Fig. 6. Again the dielectric loss tangent decreased with increase in frequency for each sample. All the samples exhibit dispersion due to the Maxwell–Wagner interfacial type polarization in agreement with Koop's phenomenological theory [14–18]. The dielectric loss tangent is greater at low frequency and small at high frequency. Iwauchi [19] pointed out that there is a strong correlation between the dielectric behavior and the conduction mechanism in ferrites. The conduction in ferrites is considered to
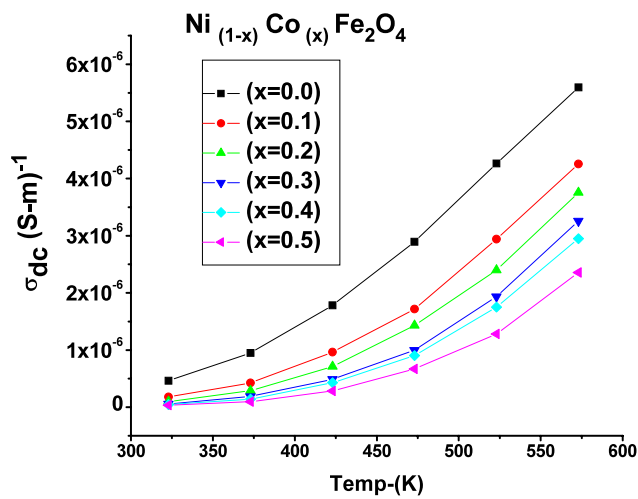
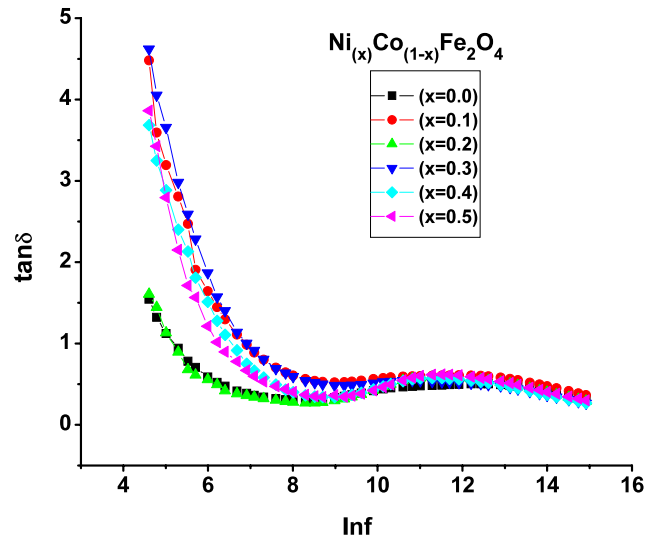**Fig. 4** Graph of dc conductivity as a function of temperature for various compositions
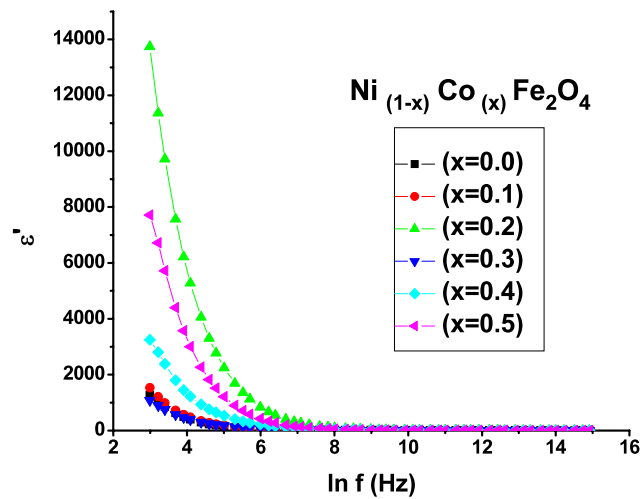
Fig. 5 Frequency dependence of dielectric constant (ε') for $Ni_{1-x}Co_xFe_2O_4$ nanoferrites

Fig. 6 Dielectric loss tangent ($\tan\delta$) as a function of frequency of $Ni_{1-x}Co_xFe_2O_4$ nanoferrites

Fig. 7 Graph of ac conductivity as a function of frequency for various concentrations of cobalt

be due to the hopping of electron between Fe ions in different valence states +2 and +3 over the octahedral sites.
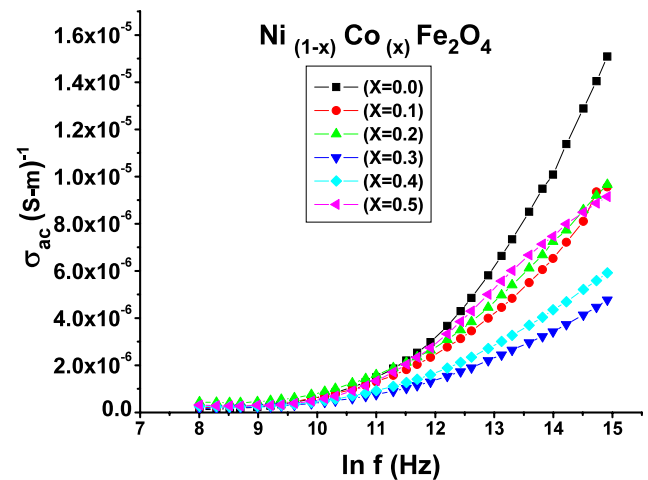
Figure 7 shows that σ_{ac} rises with the rise in the frequency, which is in agreement with the reports [20, 21]. The conductivity of ferrites, in general, depends on the density, porosity, grain size, grain boundary and chemical com- position of sample [8, 22].

3 Conclusions

(1) Co-doped spinel ferrites $Ni_{1-x}Co_xFe_2O_4$ nano ferrites were successfully prepared by the co-precipitated method.

(2) XRD analyses showed the presence of single spinel phase.

(3) The lattice parameters as well as the porosity were found to decrease with increase in Co concentration (x).

(4) The density and grain size increased with the increase of the cobalt concentration (x).

(5) Temperature-dependent dc electrical resistivity of the studied samples showed a semiconductor-like behavior.

(6) It is noticed that σ_{dc} increases with a rise in temperature.

(7) The dielectric constant (ε') and dielectric loss tangent ($\tan\delta$) showed a decreasing trend with increasing field frequency.

(8) The σ_{ac} rises with the rise in the frequency.

References

1. Naeem, M., Shah, N.A., Gul, I.H., Maqsood, A.: J. Alloys Compd. **487**, 739 (2009)
2. Kim, W.C., Kim, S.J., Lee, S.W., Kim, C.S.: J. Magn. Magn. Mater. **226**, 1418 (2001)
3. Wang, H.W., Kung, S.C.: J. Magn. Magn. Mater. **270**, 230 (2004)
4. Murthy, S.R.: Bull. Mater. Sci. **24**, 379 (2001)
5. Rezlescu, N., Rezlescu, E., Rezlescu, L., Popa, P.D., Paniscu, C., Craus, M.L.: Mater. Res. Bull. **33**, 915 (1998)
6. Rezlescu, N., Rezlescu, E., Rezlescu, L., Popa, P.D., Paniscu, C., Craus, M.L.: J. Magn. Magn. Mater. **182**, 199 (1998)
7. George, M., Nair, S.S., John, A.M., Joy, P.A., Anantharaman, M.R.: J. Phys. D: Appl. Phys. **39**, 900 (2006)
8. Gul, I.H., Abbasi, A.Z., Amin, F., Rehman, M.A., Maqsood, A.: J. Magn. Magn. Mater **311**, 494 (2007)
9. Smit, J., Wijin, H.P.J.: Ferrites. Wiley, New York (1959)
10. Berchmans, L.J., Selvan, R.K., Kumar, P.N.S.: J. Magn. Magn. Mater. **279**, 103 (2004)
11. Mott, N.F., Davis, E.A.: Electronic Proc. in Non-Cryst. Mat. Oxford, London (1979)
12. Verwey, E.J.W., Boer, F.De., Vsanten, H.H.: J. Chem. Phys. **161**, 1091 (1948)
13. El-Sayed, A.M.: Mater Chem. Phys. **82**, 583 (2003)
14. Kale, G.M., Asokan, T.: Appl. Phys. Lett. **62**, 19 (1993)
15. Austin, I.G., Mott, N.F.: Adv. Phys. **18**, 41 (1969)
16. Maxwell, J.C.: A Treatise on Elec. and Magn., vol. 2. Oxford, New York (1954)
17. Koops, C.G.: Phys. Rev. **83**, 121 (1951)
18. Wagner, K.W.: Ann. Phys. **40**, 817 (1913)
19. Iwauchi, K.: Jpn. J. Appl. Phys. **10**, 1520 (1971)
20. Batoo, K.M., Kumar, S., Lee, C.G., Current, A.: Appl. Phys. **9**, 826 (2009)
21. Ajmal, M., Maqsood, A.: Mat. Lett. **62**, 2077–2080 (2008)
22. Gul, I.H., Ahmed, W., Maqsood, A.: J. Magn. Magn. Mater. **320**, 270 (2008)